de Haas–van Alphen Effect in n-Type Bi_2Te_3†

R. B. MALLINSON AND J. A. RAYNE
Carnegie-Mellon University, Pittsburgh, Pennsylvania 15213

AND

R. W. URE, JR.
Westinghouse Research Laboratories, Pittsburgh, Pennsylvania 15235

(Received 5 June 1968)

The de Haas–van Alphen (dHvA) effect has been measured in n-type Bi_2Te_3 with carrier concentrations ranging from 9×10^{17} to 2.4×10^{19} cm^{-3}. Below 5×10^{18} cm^{-3}, the conduction-band minima can be fitted to a six-ellipsoid model, the parameters of which differ considerably from those inferred from magnetoresistance experiments. The carrier density computed from the volume of the ellipsoids agrees well with that obtained from the limiting high-field Hall coefficient at 4.2°K. At higher concentrations there is a large discrepancy between the two estimates of carrier density. The presence of a low-mobility high-mass band, lying 30 meV above the ellipsoidal minima, is postulated to explain the difference. The existence of this second band or of an anisotropic relaxation time are possible explanations of the discrepancy between the ellipsoidal parameters deduced from the dHvA and transport measurements.

I. INTRODUCTION

BISMUTH telluride (Bi_2Te_3) is a semiconducting compound with a simple rhombohedral structure, which can be made either n or p type. Several review articles discussing its properties are available.[1–3] Prior information on the nature of the conduction band of this compound has been inferred from magnetoresistance[4] and Faraday rotation[5] experiments, assuming an isotropic relaxation time for electron scattering. From the analysis of these data, it has been concluded that the conduction band is multivallied with six ellipsoidal minima.

In this paper, we report the results of extensive measurements of the de Haas–van Alphen (dHvA) effect, obtained by the torque-balance method,[6] on samples of n-type Bi_2Te_3 having a wide range of carrier concentrations. Preliminary data have been published previously.[7,8] These experiments show that at carrier concentrations of less than 5×10^{18} cm^{-3} the conduction band can be described by the six-valley ellipsoid model. However, the shape and orientation of the ellipsoids are considerably different from those derived from magnetoresistance measurements The carrier density computed from the volume of the ellipsoids agrees well with that obtained from the limiting high-field Hall coefficient at 4.2°K. At higher carrier concentrations, the carrier density computed from the ellipsoids is much lower than that obtained from the Hall data. It is concluded that the reason for this discrepancy is the existence of a low-mobility high-mass conduction band lying 30 meV above the ellipsoidal minima.

II. THEORY

A. dHvA Effect

From the theory of the dHvA effect,[6] it is known that for a degenerate assembly of electrons the free energy F and the torque $C=-\partial F/\partial\theta$ are oscillatory functions of the inverse magnetic field $(1/H)$. The fundamental frequency of these oscillations, $f(1/H)$, is related to an extremal area of the Fermi surface by

$$A_{\text{ext}}=(2\pi e/ch)f(1/H). \tag{1}$$

It is readily demonstrated that the expression for the oscillatory component of torque involves the factor $dA/d\theta$, which vanishes for anisotropic surfaces when the field is along symmetry directions. Thus, measurements of the dHvA effect by this method are not possible close to certain sample orientations. In the present instance, the technique is nevertheless very useful for measuring the very low frequencies expected from the conduction band of n-type Bi_2Te_3.

The equation for the amplitude of the dHvA oscillation in torque contains the temperature factor $x/\sinh x$, where $x=2\pi^2\kappa T/\beta^*H$ and $\beta^*=eh/m^*c$ is the effective double Bohr magneton. Thus, the effective mass m^*, defined by the usual relation $m^*=\hbar^2/2\pi(dA_{\text{ext}}/dE)$, can be obtained by measuring the temperature dependence of these oscillations. For $x\gg1$, the factor $x/\sinh x$ reduces to xe^{-x} and m^* can be determined from the slope of a plot of $\ln(C/T)$ versus T at fixed field. However, in many of our measurements the condition $x\gg1$ is

† Work supported in part by the National Science Foundation.

[1] J. R. Drabble, in *Progress in Semiconductors*, edited by A. F. Gibson and R. E. Burgess (John Wiley & Sons, Inc., New York, 1963), Vol. 7, p. 45.

[2] R. W. Ure, Jr., in *Thermoelectricity: Science and Engineering*, edited by R. R. Heikes and R. W. Ure, Jr. (Interscience Publishers, Inc., New York, 1961), p. 414.

[3] H. J. Goldsmid, in *Materials Used in Semiconductor Devices*, edited by C. A. Hogarth (Interscience Publishers, Inc., New York, 1965), p. 165.

[4] J. R. Drabble, R. D. Groves, and R. Wolfe, Proc. Phys. Soc. (London) **71**, 430 (1958), hereafter referred to as DGW.

[5] I. G. Austin, Proc. Phys. Soc. (London) **76**, 169 (1960).

[6] See, e.g., D. Shoenberg, in *Progress in Low Temperature Physics*, edited by C. J. Gorter (North-Holland Publishing Co., Amsterdam, 1957), Vol. 2, Chap. 8.

[7] R. B. Mallinson, J. A. Rayne, and R. W. Ure, Jr., Phys. Letters **19**, 545 (1965).

[8] R. B. Mallinson, J. A. Rayne, and R. W. Ure, Jr., Phys. Letters **24A**, 713 (1967).

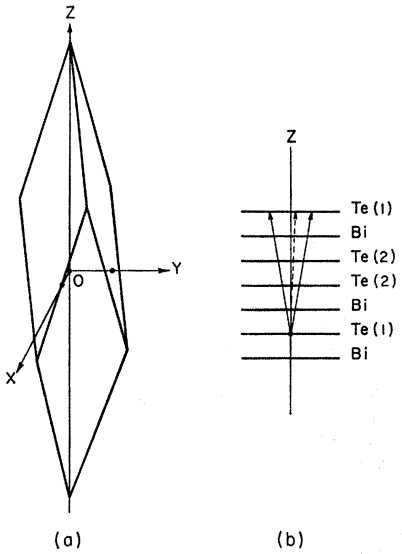

FIG. 1. (a) Schematic representation of rhombohedral unit cell for Bi_2Te_3 showing the binary, bisectrix, and trigonal axis Ox, Oy, and Oz; (b) arrangement of atoms within unit cell.

not satisfied. In this case, the temperature dependence of the torque can be expressed in the form

$$\ln\frac{C}{T}=-\frac{2\pi^2\kappa T}{\beta^* H}-\ln\left[1-\exp\left(-\frac{4\pi^2\kappa T}{\beta^* H}\right)\right]+\text{const.} \quad (2)$$

This equation can be solved iteratively, since the second term on the right side is small compared to the first.

B. Band Structure

Bi_2Te_3 has a simple rhombohedral structure, corresponding to the space group $R\bar{3}m$, with one molecule per unit primitive cell. The atoms are arranged in layers with only one kind (Bi or Te) of atom in each layer, as shown schematically in Fig. 1. The bonding between the atoms on the two adjacent Te layers [Te(2)] is weaker than that between the other atoms in the crystal and is responsible for the pronounced cleavage of the crystal. The rhombohedral lattice parameter a and the rhombohedral angle α are listed in Table I. These constants have been extrapolated to 0°K using the expansion data of Francombe.[9]

TABLE I. Crystallographic data for Bi_2Te_3.

Symbol	Magnitude	Magnitude (units of b)	Definition
a	10.418 Å		Rhombohedral vector at 0°K
α	24°12′40″		Rhombohedral angle at 0°K
b	1.6731 Å^{-1}	1.0000	Reciprocal-lattice vector
β	61°30′37″		Rhombohedral angle for reciprocal lattice
V	169.11 Å^3		Unit-cell volume
ΓA	0.8366 Å^{-1}	0.5000	$\frac{1}{2}$(100) spacing
ΓD	0.8556 Å^{-1}	0.5114	$\frac{1}{2}$(110) spacing
ΓZ	0.3108 Å^{-1}	0.1858	$\frac{1}{2}$(111) spacing
θ_1	7°6′50″		Angle between ΓA and ΓY
θ_2	14°0′50″		Angle between ΓD and ΓY

The symmetry elements of the $R\bar{3}m$ space group are (a) one threefold rotation axis, (b) three reflection planes containing the threefold axis and making 120° angles with each other, (c) three twofold rotation axes perpendicular to the threefold axis and lying midway between the reflection planes, and (d) a center of inversion. The basis vectors for the rhombohedral unit cell lie in the reflection planes. In subsequent discussion, it will be convenient to use two coordinate systems. The first is a Cartesian system with the z or 3 axis along the threefold rotation axis, the x or 1 axis (the binary direction) along a twofold rotation axis, and the y or 2 axis (the bisectrix direction) in a reflection plane.[10] The second system is a hexagonal coordinate system with the 1, 2, and 3 axes along the twofold axes and the 4 axis along the threefold rotation axis. In this system the binary directions are $\langle 2\bar{1}\bar{1}0\rangle$ and the bisectrix directions are $\langle 10\bar{1}0\rangle$.

Figure 2 shows the relevant Brillouin zone, which is bounded by $\{10\bar{1}1\}$, $\{1\bar{1}02\}$, and $\{0001\}$ faces, together with the symmetry points labeled according to the notation of Koster.[11] It is to be noted that the assumed positive direction of the bisectrix shown in Fig. 2 is opposite to that given by Drabble.[1] Table I gives the principal dimensions of the Brillouin zone computed from the extrapolated values of a and α. The zone is similar to that in bismuth, which is also rhombohedral, but is very much more distorted because of the large unit-cell dimension along the trigonal direction.

Drabble and Wolfe[12] have listed a number of types of electron constant-energy surfaces consistent with the crystal symmetry, the most general being a 12-ellipsoidal-valley model in which one valley may have an arbitrary position and arbitrary orientation in **k** space. However, Drabble, Groves, and Wolfe[4] were able to fit their magnetoresistance data with a more restricted

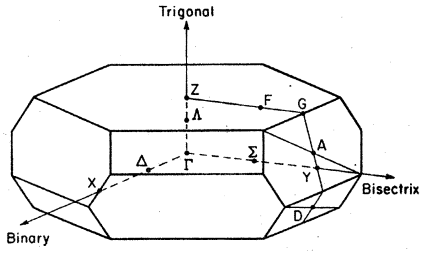

FIG. 2. Brillouin zone for Bi_2Te_3 showing location of symmetry points. The scale of the drawing has been exaggerated along ΓZ for the purpose of clarity.

[9] M. H. Francombe, Brit. J. Appl. Phys. **9**, 415 (1958).
[10] This system is the one commonly used for bismuth, which has the same symmetry as Bi_2Te_3. It differs from the system used in Refs. 4 and 12 but is similar to the system used in Ref. 1.
[11] G. F. Koster, in *Solid State Physics*, edited by F. Seitz and D. Turnbull (Academic Press Inc., New York, 1957), Vol. 5.
[12] J. R. Drabble and R. Wolfe, Proc. Phys. Soc. (London) **B69**, 1101 (1956).

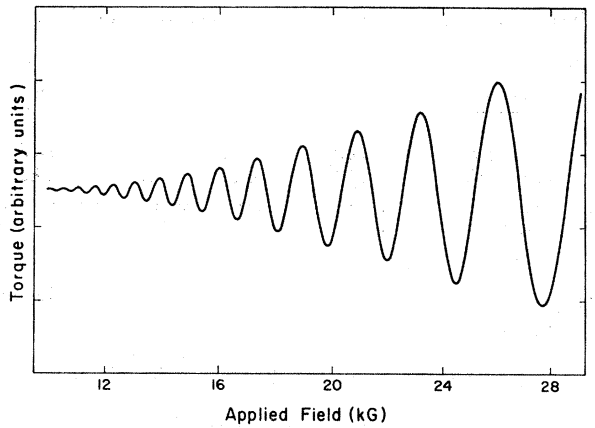

FIG. 3. Typical dHvA data obtained for n-type Bi_2Te_3 with $n_H=6.2\times10^{18}$ cm^{-3}. The suspension is nominally along the trigonal axis and the field is directed close to the binary axis.

model, viz., six ellipsoids centered on the reflection planes and having one axis perpendicular to the reflection plane. The three axes of the representative ellipsoid have arbitrary length and the ellipsoid may be tilted so that none of its axes are parallel to the trigonal axis of the crystal.

The band structure of Bi_2Te_3 has been calculated by Pincherle and Lee[13] using the augmented plane-wave (APW) method. These calculations do not give an energy gap without the introduction of spin-orbit coupling, which of course must be important, since both bismuth and tellurium have high atomic numbers. In this work, the introduction of spin-orbit effects by an approximate perturbation technique produces a direct gap between the conduction and valence bands, with the minimum in the conduction band at the points D of the Brillouin zone. Thus the model predicts the conduction band used by DGW,[4] except for the fact that there are only three minima instead of six. There are, however, relatively large uncertainties of about 0.5 eV in the calculated bands and hence it is entirely possible that the minima could in fact occur near D, giving rise to a conduction band with six valleys.[13a] It is of interest that the magnetoresistance data cannot distinguish between a three- or six-valley model, but only the latter is consistent with Faraday-rotation data.[5]

III. EXPERIMENT

dHvA measurements on samples of n-type Bi_2Te_3 have been made at fields up to 29 kG, using an automatic-recording torque balance.[14] To improve the signal-to-noise ratio, it is convenient to use an integrating operational amplifier followed by a passive RC differentiating device in the recording circuit. These circuits are quite conventional and do not merit detailed description. For suspensions other than that along the trigonal axis, there is a large static component of torque. To eliminate its effect, a differential-input operational amplifier is included in the feedback circuit. This amplifier combines the signal resulting from the susceptibility of the sample with an opposing signal proportional to the square of the applied field. By suitable choice of the magnitude of this bucking signal, the effects of the static torque can be eliminated over the field range used in the experiments. A typical recording trace for a trigonal axis suspension of a sample with carrier concentration $n_H=6.2\times10^{18}$ cm^{-3} is shown in Fig. 3.

The samples are spark-cut from ingots of n-type Bi_2Te_3 grown by a horizontal loaded-zone technique from 99.999% pure starting material. Bi_2Te_3 grown from a stoichiometric melt is p type with a hole concentration of about 2×10^{19} cm^{-3}. It can be made n type by doping with an n-type dopant such as iodine or by introducing excess tellurium into the crystal by growing from a melt containing more than 62.7 at.% of this constituent.[15] In the first case, the samples are compensated and the mobility at He temperatures is much lower than in samples prepared by the second technique.[16,17] Since samples with high carrier mobility are required in order to observe the dHvA effect, all samples have been grown from melts containing excess Te and no impurity doping. Electron Hall mobilities as high as 180 000 cm^2/V sec can be obtained in samples prepared by this technique.[16]

To determine the carrier density, the Hall coefficients have been measured at high magnetic fields on specimens cut from the ingot adjacent to each dHvA sample. There are two Hall coefficients for crystals having the symmetry $R\bar{3}m$, viz., ρ_{123} and ρ_{312}. These coefficients are obtained with the magnetic field perpendicular and parallel to the cleavage plane, respectively, and the sample current parallel to the cleavage plane and perpendicular to the magnetic field. The carrier density is related to the Hall coefficient by

$$n_H=rB_{ijk}/e\rho_{ijk}, \tag{3}$$

where r is a factor that depends on the energy dependence of the carrier scattering and the degree of degeneracy, and B_{ijk} depends on the anisotropy of the band structure and relaxation time. In many semiconductors r and B_{ijk} are close to unity, even at low fields. However, DGW[4] find a value of $B_{123}=0.326$, which, for our purposes is very different from unity. For magnetic fields large enough that $\omega\tau\gg1$, where ω

[13] P. M. Lee and L. Pincherle, Proc. Phys. Soc. (London) 81, 461 (1963).

[13a] *Footnote added in proof.* Recent pseudopotential calculations by F. Borghese and E. Donato [Nuovo Cimento 53B, 283 (1968)] confirm this assignment.

[14] J. H. Condon and J. A. Marcus, Phys. Rev. 134, A446 (1964).

[15] C. B. Satterthwaite and R. W. Ure, Jr., Phys. Rev. 108, 1164 (1957).

[16] R. W. Ure, Jr., in *Proceedings of the International Conference on the Physics of Semiconductors, Exeter* (The Institute of Physics and The Physical Society, London, 1962), p. 659.

[17] B. Yates, J. Electron. Control 6, 26 (1959).

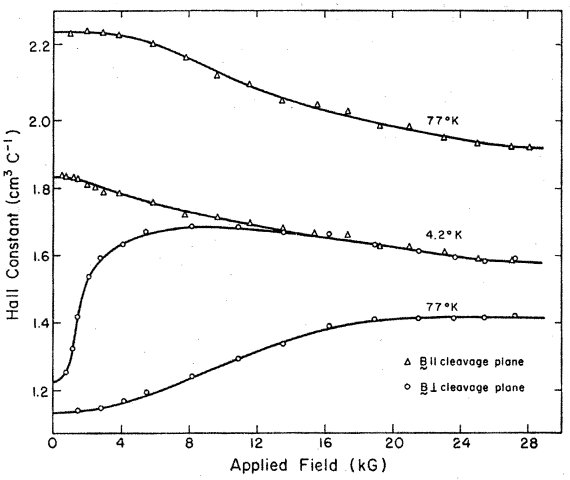

FIG. 4. Typical Hall data for n-type Bi_2Te_3 showing the variation of ρ_{123} and ρ_{312} with field at both nitrogen and helium temperatures. The carrier concentration obtained from the limiting high-field Hall constant at 4.2°K is 3.7×10^{18} cm^{-3}.

is the relevant cyclotron frequency and τ is the carrier relaxation time, these parameters become $r=B_{123}=B_{312}=1$. Therefore, carrier concentrations have been calculated from Hall coefficients measured at 4.2°K and 28 kG. In all cases, the condition $\omega\tau\gg1$ is amply satisfied under these conditions. Data for a low-carrier-concentration sample are shown in Fig. 4, which clearly illustrates the equality of the saturation Hall coefficients. At higher carrier densities, the coefficients still exhibit saturation but the limiting values differ by as much as 15% because of unavoidable specimen inhomogeneity.

IV. RESULTS AND DISCUSSION

Figure 5 shows the dHvA frequency $f(1/H)$ as a function of the magnetic-field direction for a sample with $n_H=3.7\pm0.1\times10^{18}$ cm^{-3}, the suspension being along the trigonal axis [0001]. The data exhibit sixfold symmetry, characteristic of either a three- or six-valley conduction band. Figures 6 and 7 show the variation of $f(1/H)$ with field direction for suspension of the sample along a binary and a bisectrix axis, respectively.

From Fig. 5, it is evident that the minimum extremal area for each valley occurs with the field lying in a mirror plane. Thus the equation of the representative

TABLE II. Comparison of ratios α_{ij}/α_{22} obtained from magnetoresistance and dHvA data.

Expt.	α_{11}/α_{22}	Ratio α_{33}/α_{22}	α_{23}/α_{22}	Tilt angle (deg)
MR	0.097	0.135	0.222[a]	±14[b]
dHvA (low n)	7.94	1.57	0.352	25.4
dHvA (high n)	8.21	1.67	0.428	26.0

[a] There is an apparent misprint in the value of α_{23} in Table III of Ref 5.
[b] The sign of the tilt angle is not determined in the magnetoresistance experiments.

TABLE III. Comparison of components α_{ij} of inverse effective-mass tensor obtained from magnetoresistance and dHvA data.

Expt.	α_{11}	α_{22}	α_{33}	α_{23}
MR	3.9	40	5.4	8.9
dHvA (low n)	34.6	4.35	6.86	1.53
dHvA (high n)[a]	35.1	4.27	7.13	1.83

[a] Computed for $m_{av}^*=0.102\ m_0$ obtained from sample with $n_H=3.7\times10^{18}$ cm^{-3}.

ellipsoid which is located in the y-z plane must be of the form

$$\alpha_{11}k_1^2+\alpha_{22}k_2^2+\alpha_{33}k_3^2+2\alpha_{23}k_2k_3=2m_0E_F/\hbar^2, \quad (4)$$

where α_{ij} are the components of the inverse effective-mass tensor and E_F is the Fermi energy. The corresponding tilt angle of the ellipsoid is given by the expression

$$\tan2\theta=-2\alpha_{23}/(\alpha_{22}-\alpha_{33}). \quad (5)$$

It is easily shown from Eq. (1) that the dHvA frequency arising from this ellipsoid, for a field along the direction specified by the direction cosines $(\lambda_1,\lambda_2,\lambda_3)$, is

$$1/f=(e\hbar/cm_0E_F)[(\alpha_{22}\alpha_{33}-\alpha_{23}^2)\lambda_1^2+\alpha_{11}\alpha_{33}\lambda_2^2+\alpha_{11}\alpha_{22}\lambda_3^2-2\alpha_{11}\alpha_{23}\lambda_2\lambda_3]^{1/2}. \quad (6)$$

Corresponding equations are readily derived for the other ellipsoids from the requirements of crystal symmetry.

A computer program has been developed to fit the experimental data to these equations, allowing for orientation errors of the suspension axis (and hence the field rotation plane) relative to the principal axes of the crystal. This program is a multivariate least-squares analysis in the parameters α_{11}, α_{22}, α_{33}, α_{23}, and those specifying the misorientation of the suspension axis. The full curves in Figs. 5–7 are the final results of this analysis. It is clear that the fit to the data is within

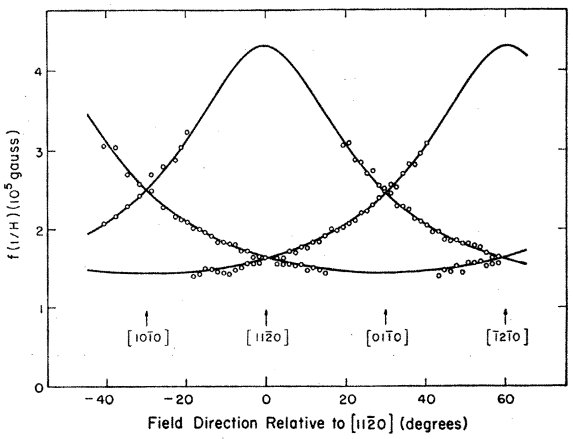

FIG. 5. Variation of $f(1/H)$ as a function of field direction for a sample of n-type Bi_2Te_3 with $n_H=3.7\times10^{18}$ cm^{-3} suspended along the trigonal axis. The full curves are a theoretical fit to the data using a six-ellipsoid model.

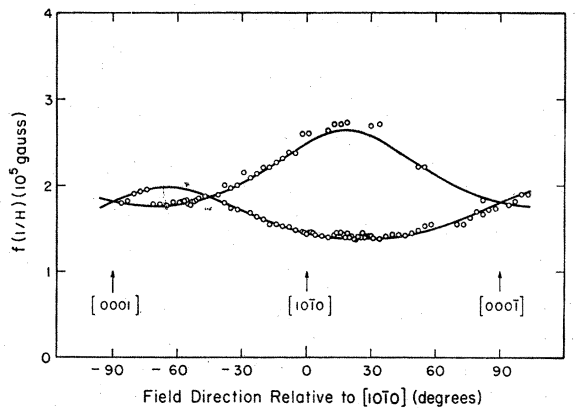

FIG. 6. Variation of $f(1/H)$ as a function of field direction for a sample of n-type Bi_2Te_3 with $n_H=3.7\times10^{18}$ cm^{-3} suspended along the binary axis. The full curves are a theoretical fit to the data using a six-ellipsoid model.

experimental error, so that to this accuracy the hypothesis of ellipsoidal valley minima appears to be correct. The resulting ratios of α_{ij} relative to α_{22} are summarized in Table II, together with those computed by DGW from their magnetoresistance data. There is clearly marked disagreement between the two sets of parameters, as can be seen from Fig. 8, which shows a schematic representation of the ellipsoids for each model. In both cases the ellipsoids are almost spheroidal, with two of the axes being nearly equal and the other considerably smaller. The magnetoresistance data indicate that the ellipsoids are compressed in a direction almost parallel to the bisectrix, while the present data indicate a compression almost parallel to the binary axis. There is also a disagreement in the magnitude ot the tilt angle, the value obtained from this work being 25.4° compared to 14° obtained from the transport measurements. In this connection it is to be noted that the latter do not determine the sign of the tilt angle in contrast to the dHvA data, which show that the sense of the tilt is as shown in Fig. 8(b).

The absolute values of the constants α_{ij} can be determined by measuring the effective mass for a given extremal orbit on the principal ellipsoid. From Eq. (6),

TABLE IV. Crossing frequencies for n-type Bi_2Te_3 as a function of n_H, the carrier density computed from Hall data. The axis of suspension is the trigonal axis [0001], while the magnetic field directions are the bisectrix [10$\bar{1}$0] and binary [2$\bar{1}\bar{1}$0] directions.

n_H (10^{18} cm^{-3})	$f(1/H)$ (10^5 G) [10$\bar{1}$0]	[2$\bar{1}\bar{1}$0]	Ratio $f_{[10\bar{1}0]}/f_{[2\bar{1}\bar{1}0]}$
0.90±0.05	0.79	0.50	1.58
1.9 ±0.1	1.38	0.90	1.54
3.7 ±0.1	2.50	1.55	1.61
6.2 ±0.3	3.20	2.10	1.52
8.2 ±0.5	3.20	2.10	1.52
12 ±1.0	3.50	2.30	1.52
16 ±1.0	3.93	2.58	1.52
24 ±1.5	4.15	2.65	1.56

it is easily seen that, for the field along $(\lambda_1,\lambda_2,\lambda_3)$, the effective mass is given by

$$m^*=m_0[(\alpha_{22}\alpha_{33}-\alpha_{23}^2)\lambda_1^2+\alpha_{11}\alpha_{33}\lambda_2^2+\alpha_{11}\alpha_{22}\lambda_3^2 -2\alpha_{11}\alpha_{23}\lambda_2\lambda_3]^{-1/2}. \quad (7)$$

This expression can then be solved for the value of α_{22} using the previously determined ratios of α_{ij} to α_{22}. For the [0001] suspension, effective masses have been determined for the field directed both along the binary and bisectrix directions. The resulting experimental values of effective mass are consistent with Eq. (6) and give the components of α_{ij} shown in Table III. Also listed are the corresponding values obtained from combining the data of DGW with the infrared Faraday-rotation data of Austin[2]; there is, of course, the disagreement mentioned previously. It is of interest, however, that the average effective mass derived from the optical measurements, viz.,

$$m_{av}^*=m_0[\alpha_{11}(\alpha_{22}\alpha_{33}-\alpha_{23}^2)]^{-1/3}, \quad (8)$$

gives a value of $m_{av}^*=0.12m_0$, which is reasonably close to the figure $m_{av}^*=0.101m_0$ obtained from dHvA data.

The carrier concentration corresponding to the ellipsoidal conduction minima is given by

$$n_E=(s/3\pi^2)[A_1A_2A_3/\pi^3]^{1/2}, \quad (9)$$

where A_1, A_2, and A_3 are the principal extremal areas of each ellipsoid and s is the number of valley minima. If s is assumed to be six, then the data for this sample give $n_E=3.7\pm0.05\times10^{18}$ cm^{-3}, which agrees with the value of $n_H=3.7\pm0.1\times10^{18}$ cm^3. Thus the dHvA data are consistent only with a six-ellipsoid model, which in the context of the theoretical calculations of Pincherle and Lee[13] implies that the minima in the conduction band are located near the points D in the Brillouin zone.

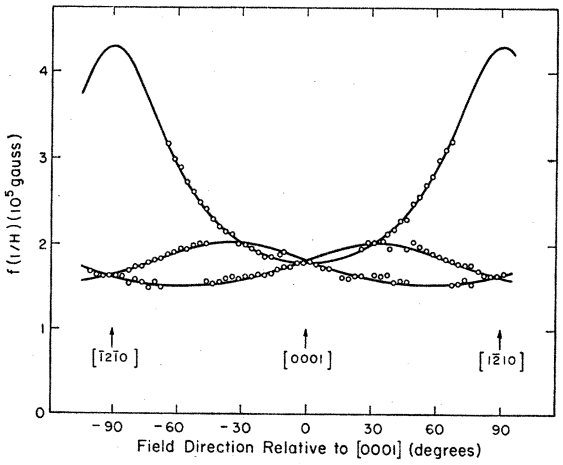

FIG. 7. Variation of $f(1/H)$ as a function of field direction for a sample of n-type Bi_2Te_3 with $n_H=3.7\times10^{18}$ cm^{-3} suspended along the bisectrix axis. The full curves are a theoretical fit to the data using a six-ellipsoid model.

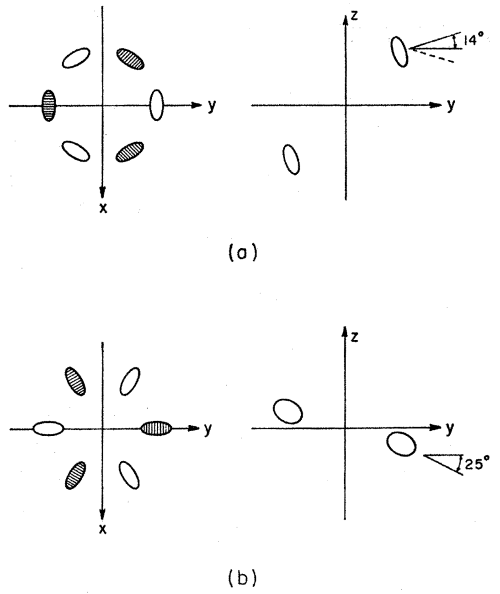

FIG. 8. Schematic representation of ellipsoid model fitted to (a) magnetoresistance data and (b) dHvA measurements. The location of the ellipsoids in the mirror planes has no significance.

It is noteworthy that the analysis of the optical data[5] gives $s=5.1$, which also strongly suggests a six-valley model consistent with the requirements of crystal symmetry.

The dHvA effect in n-type Bi_2Te_3 has been measured up to a maximum carrier density of $n_H=2.4\times10^{19}$ cm^{-3}. The observed oscillation frequencies for two magnetic-field directions, with a trigonal axis suspension, are shown in Table IV. The fact that the ratio of the frequencies in the two directions is independent of carrier concentration indicates that the ellipsoid shape is independent of carrier concentration over the range from 9×10^{17} to 2.4×10^{19} cm^{-3}. Figures 9–11 show complete data obtained for a sample with $n_H=1.2\pm0.1\times10^{19}$ cm^{-3}, together with the curves giving the best analytical fit to a six-ellipsoid model. Except for the suspension along a binary axis, the agreement between the model and the experimental data is within the estimated errors. The discrepancy between the data points and the theoretical curves shown in Fig. 10 is presumably due to a slight nonellipsoidal shape of the constant-energy surfaces at this high carrier concentration. The ratios of the coefficients α_{ij}/α_{22} are given in Table II, which shows that they do not vary appreciably with carrier density and hence that the assumption of a rigid ellipsoidal conduction band is approximately correct. For higher carrier concentrations, where it is difficult to obtain complete dHvA data, this assumption has been used to infer n_E from the data for a trigonal axis of suspension only. It is believed that the error resulting from this assumption is small, since the carrier concentration computed in this way for the specimen with $n_H=1.2\times10^{19}$ cm^{-3} differs by only a few percent from that computed directly from the measured principal areas, as can be seen from Fig. 12.

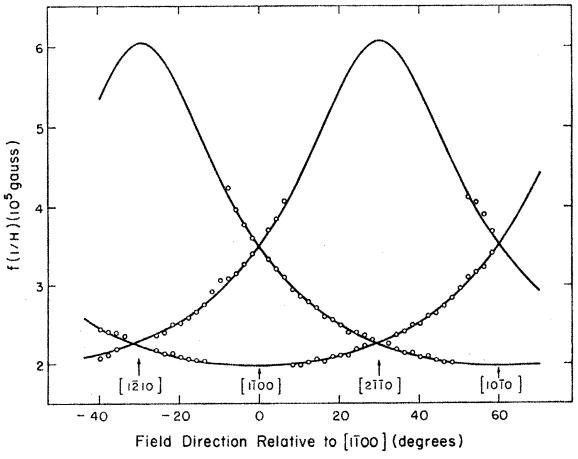

FIG. 9. Variation of $f(1/H)$ as a function of field direction for a sample of n-type Bi_2Te_3 with $n_H=1.2\times10^{19}$ cm^{-3} suspended along the trigonal axis. The full curves are a theoretical fit to the data using a six-ellipsoid model.

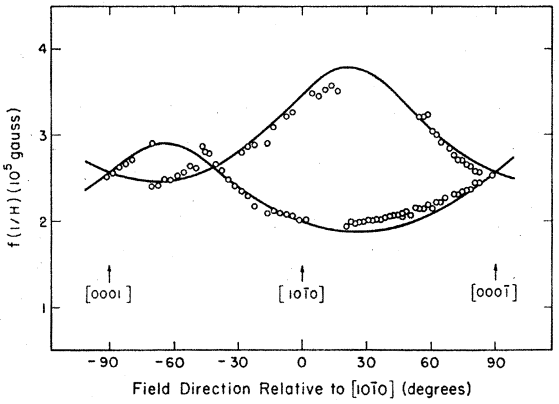

FIG. 10. Variation of $f(1/H)$ as a function of field direction for a sample of n-type Bi_2Te_3 with $n_H=1.2\times10^{19}$ cm^{-1} suspended along the binary axis. The full curves are a theoretical fit to the data using a six-ellipsoid model.

The variation of n_E and n_H, computed from the dHvA and Hall data, respectively, is shown in Fig. 12. Note that the scales on the ordinate and abscissa are different and that the solid line represents the relation $n_E=n_H$. Up to about $n_H=5\times10^{18}$ cm^{-3} the carrier concentrations determined by the two measurements agree quite well, but beyond this value there is an increasing difference between the two densities. Thus for the sample with $n_H=1.2\pm0.1\times10^{19}$ cm^{-3}, the corresponding value of n_E is $6.3\pm0.5\times10^{18}$ cm^{-3}. The uncertainty in the former figure results from sample inhomogeneity, while in the latter figure it represents the uncertainty arising from the nonellipsoidal shape of the conduction-band minima. Clearly the disagreement is well outside the combined error limits.

It is believed that the reason for this disagreement is the existence of a high-mass low-mobility band lying slightly higher in energy than the ellipsoidal minima discussed above. At higher carrier concentrations, electrons begin to fill this heavy-mass band, so that the Fermi energy increases more slowly as a function of n_H and the rate of increase in n_E is correspondingly reduced. The mobility of this second group of carriers must, of course, be low enough that they do not give an observable dHvA signal at the fields used in these experiments but sufficiently large that they do contribute significantly to the measured Hall voltage. The dashed line in Fig. 12 is a fit of the data to an assumed parabolic second band starting at the point X, and lying 30 meV above the ellipsoidal valleys. This fit gives an average effective mass of $m^*=1.5\ m_0$ for the second group of carriers, assuming that they are contained in a single valley and that the high-field Hall coefficient gives a correct value for the total carrier concentration.[17a]

From the present data, it is not possible to determine whether the second group of carriers is contained within a separate band or another local minimum of that containing the first group. Existing calculations of the band structure are not sufficiently precise to give any information on this point. The existence of a higher conduction band has been proposed to explain various features of previous measurements of transport properties in Bi_2Te_3.[16–19] However, we believe that the present work gives the first strong evidence for the presence of this second conduction band.

There are two reasons why the dHvA and magnetoresistance measurements give widely different parameters for the shape of the ellipsoids: (a) The samples used by DGW had a carrier concentration of about 1×10^{19}. (DGW give Hall-coefficient data at 77°K and at low magnetic field. This value of n was calculated by noting from Fig. 4 that the high-field 4.2°K Hall coefficient is roughly equal to the average of the two low-field Hall coefficients at 77°K.) Thus there will be carriers in the upper conduction band in their samples and these carriers will affect the magnetoresistance measurements. (b) The magnetoresistance is determined both by the anisotropy of the constant energy surfaces and by the anisotropy of the relaxation time τ. In order to analyze their data, DGW assumed that τ was isotropic. Since the dHvA data are not affected by any anisotropy in τ, there will be a difference between the magnetoresistance and the dHvA results if τ is anisotropic. Transport measurements on low-carrier-concentration samples are being made to eliminate effect of (a) and to evaluate the anisotropy of τ.

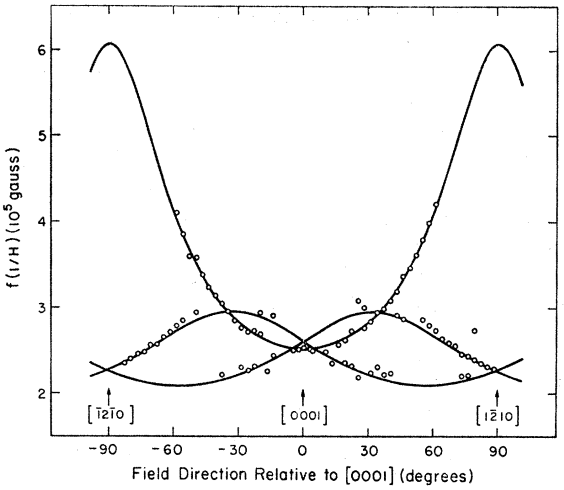

FIG. 11. Variation of $f(1/H)$ as a function of field direction for a sample of n-type Bi_2Te_3 with $n_H=1.2\times10^{19}$ cm^{-3} suspended along the bisectrix axis. The full curves are a theoretical fit to the data using a six-ellipsoid model.

Goldsmid[20] has measured the magnetoresistance at 77°K in a sample of carrier concentration about 6×10^{19}. He finds that the shape of the ellipsoids deduced from these data varies with carrier concentration. However, this effect is more likely a result of the increasing importance of the upper conduction band as the carrier concentration is increased.

V. CONCLUSIONS

dHvA data have been obtained for n-type Bi_2Te_3 over a wide range of carrier concentrations. These measure-

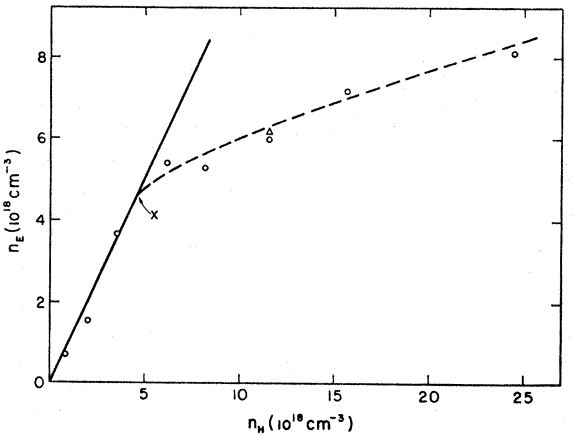

FIG. 12. Dependence of n_E, the carrier concentration derived from the dHvA data, on n_H, the carrier concentration determined from the limiting high-field Hall coefficient at 4.2°K. The full line is the relation $n_E=n_H$, while the dashed curve is a fit to the high carrier density data for a parabolic second band. This band is assumed to have a minimum corresponding to the point X. The error resulting from the assumption of a rigid conduction band is shown by the difference between the circle and triangle for $n_H=1.2\times10^{19}$ cm^{-3}.

[17a] *Footnote added in proof.* Owing to their large effective mass, these carriers would have a large temperature factor and hence would give a negligible dHvA effect at the fields used in these experiments.

[18] P. A. Walker, Proc. Phys. Soc. (London) **76**, 113 (1960).

[19] P. Drath and G. Landwehr, Phys. Letters **24A**, 504 (1967).

[20] H. J. Goldsmid, J. Appl. Phys. **32**, 2198 (1961).

ments show that the conduction band consists of six ellipsoidal minima centered on the reflection planes of the crystal. Two of the major axes of the ellipsoids lie in the reflection planes and make angles of 25° with respect to the trigonal and bisectrix directions, respectively. In addition, there is a second conduction band consisting of one or more minima lying approximately 30 meV above the first set. The shape of the constant-energy surfaces for the lower band is independent of the carrier concentration for total carrier concentrations between 9×10^{17} and 2.4×10^{19}. The average effective mass is reasonably close to that obtained from Faraday-rotation experiments.

ACKNOWLEDGMENTS

Thanks are due to Dr. G. B. Brandt for his help in making the initial measurements and to D. Zupon for his assistance in preparing the samples used in these experiments. Two of us (R.B.M. and J.A.R.) gratefully acknowledge the support of the National Science Foundation.

PHYSICAL REVIEW VOLUME 175, NUMBER 3 15 NOVEMBER 1968

Intensity of Forbidden Neutron Reflections Simulated by Multiple Bragg Reflection*

D. A. KOTTWITZ

Battelle Memorial Institute, Pacific Northwest Laboratory, Richland, Washington 99352

(Received 29 May 1968)

Exploratory measurements have been made of the intensity of several forbidden neutron reflections simulated by multiple Bragg reflection in large single crystals. The (0003) and (0001) reflections were studied in a beryllium crystal with mosaic <0.25° and the (200) in a germanium crystal with mosaic <0.02°. Double-crystal methods were used with a triple-axis spectrometer. Large amounts of order contamination were treated by means of resonance absorption filters and least-squares analysis of overdetermined equations. To minimize the effect of peculiarities of individual specimens, the results are presented as intensity ratios. Simulated reflections were observed to have 1/60 to $\frac{1}{5}$ the intensity of ordinary Bragg reflections. No conclusive evidence was found for an intrinsic component due to the forbidden reflections themselves; the Be simulations were at least 200 to 700 times, and the Ge simulations at least 15 to 60 times, more intense than the corresponding intrinsic components. Caution must be used in applying these results to other specimens.

I. INTRODUCTION

FOR several decades the phenomenon of multiple Bragg reflection (MBR) (often referred to as multiple diffraction or simultaneous reflection) has been studied experimentally and theoretically for x rays, electrons, and neutrons; an extensive literature has been reviewed recently.[1] Although a number of beneficial uses have been suggested and demonstrated, it is probably fair to say that the effect has been mostly a nuisance. This is true for both spectrometry and structure studies, in which perturbed intensities of ordinary reflections and confusing appearances of forbidden reflections may occur. In fact much recent work has dealt with the question of avoiding or minimizing the effects of MBR.

However, the possibility of producing extremely monochromatic, semiparallel beams of x rays and slow neutrons at fixed wavelengths by means of MBR in certain types of perfect single crystals has been pointed out recently.[2] The proposed method is based on effects which occur at particular crystal orientations in cases of pure "*Umweganregung*"[3]; that is, when a strongly forbidden Bragg reflection is simulated by MBR. Such high-quality beams, particularly of slow neutrons, have several potential uses in research, provided they are intense enough. Although several investigations concerned with the intensity of simulated neutron reflections have been reported,[4–6] it is difficult to relate their results to the reflectivity of large crystals, which is the basic quantity of interest in monochromatization.

The purpose of this paper is to present the results of a preliminary experimental survey of several simulated neutron reflections, the main goals of which were (1) to determine the general order of magnitude of their intensity and (2) to identify some of the more intense peaks for subsequent detailed study. The measurements

* Work performed under U. S. Atomic Energy Commission Contract No. AT(45-1)-1830.

[1] Yu. S. Terminasov and L. V. Tuzov, Usp. Fiz. Nauk **83**, 223 (1964) [English transl.: Soviet Phys.—Usp. **7**, 434 (1964)].

[2] D. A. Kottwitz, Acta Cryst. **A24**, 117 (1968).

[3] M. Renninger, Z. Physik **106**, 141 (1937).

[4] H. J. Hay, Atomic Energy Research Establishment Report No. AERE-R 2982, 1959 (unpublished).

[5] R. M. Moon and C. G. Shull, Acta Cryst. **17**, 805 (1964).

[6] R. R. Spencer, Atomic Energy Commission Research and Development Report No. IDO-17029, 1964 (unpublished).